Experience-dependent maturation of the glomerular microcircuit

Brady J. Maher, Matthew J. McGinley, and Gary L. Westbrook[1]

Vollum Institute, Oregon Health and Science University, Portland, OR 97239

Spontaneous and patterned activity, largely attributed to chemical transmission, shape the development of virtually all neural circuits. However, electrical transmission also has an important role in coordinated activity in the brain. In the olfactory bulb, gap junctions between apical dendrites of mitral cells increase excitability and synchronize firing within each glomerulus. We report here that the development of the glomerular microcircuit requires both sensory experience and connexin (Cx)36-mediated gap junctions. Coupling coefficients, which measure electrical coupling between mitral cell dendrites, were high in young mice, but decreased after postnatal day (P)10 because of a maturational increase in membrane conductance. Sensory deprivation, induced by unilateral naris occlusion at birth, slowed the morphological development of mitral cells and arrested the maturational changes in membrane conductance and coupling coefficients. As the coupling coefficients decreased in normal mice, a glutamate-mediated excitatory postsynaptic current (EPSC) between mitral cells emerged by P30. Although mitral–mitral EPSCs were generally unidirectional, they were not present in young adult Cx36$^{-/-}$ mice, suggesting that gap junctions are required for the development and/or function of the mature circuit. The experience-dependent transition from electrical transmission to combined chemical and electrical transmission provides a previously unappreciated mechanism that may tune the response properties of the glomerular microcircuit.

connexin 36 | gap junctions | mitral cells | olfactory | EPSC

The development, as well as function, of many neuronal circuits involves the interplay between chemical and electrical transmission. Spontaneous activity and sensory experience provide neural input important for circuit development (1–3). Electrical transmission may be instructive for developing circuits, because gap junctions are permeable to Ca^{2+}, small organic metabolites, and second messengers (4, 5). Gap junctions also can provide a structural blueprint for circuit formation by physically connecting neurons into cortical columns (6, 7). At a functional level, electrical synapses can synchronize spontaneous oscillations that are instructive for developing circuits (8–10, 5, 11, 12).

In the adult rodent brain, connexin (Cx)36 is responsible for the majority of electrical synapses between neurons (13, 14). The presence of gap junctions often defines functional sets of neurons; thus, creating neuronal networks (15) that synchronize neuronal activity (16–20). In the olfactory bulb, each glomerulus comprises a functional microcircuit, in which mitral cells that project their apical dendrites to the same glomerulus are electrically coupled (19, 21). Excitability within the glomerulus is influenced by glutamate release from mitral cells that leads to autoexcitation (22–26) and lateral excitation (27). Summated chemical and electrical transmission between mitral cells is important for amplification of odorant inputs from olfactory receptor neurons and correlated output to olfactory cortex (27, 28).

We report here that the impact of chemical and electrical transmission on mitral cell excitability changes dramatically during development. To assess glomerular activity, we used paired somatic and paired dendritic recordings from mitral cells during the first 5 postnatal weeks. This time window is critical for bulb development (29, 30). Simulations of a glomerular network were used to assess the relationship of the gap-junctional conductance to other membrane conductances. During this period, the coupling coefficient between mitral cells decreased because of increases in non-gap-junctional membrane conductances, and a glutamate-mediated mitral–mitral excitatory postsynaptic current (EPSC) emerged. These measures of circuit maturation were differentially affected by sensory deprivation or genetic removal of Cx36. Surprisingly, spontaneous mitral cell activity in slices from young adult mice was high in sensory-deprived animals, but nearly absent in Cx36$^{-/-}$ animals.

Results

Sensory Experience and Electrical Coupling Between Mitral Cells. We made recordings from pairs of mitral cells in slices that ranged in age from postnatal day (P)7 to 42 (Fig. 1A). In control animals, direct current injection into one cell (cell 1; −250 to −400 pA, 0.7 s) elicited a simultaneous voltage deflection in the follower cell (cell 2; Fig. 1A), consistent with electrical coupling between mitral cells that project their apical dendrite to the same glomerulus (19, 21). The coupling coefficient was high in young animals (12.4 ± 1.3%, P7–10, n = 24), and then decreased after the first postnatal week (Fig. 1B; $P < 0.0001$, Newman–Keuls 1-way ANOVA). However, substantial electrical coupling persisted in normal young adult animals (3.29 ± 0.62%, P31–40, n = 34). These values match those previously reported in P14–21 mitral cells (19, 21), indicating that coupling coefficients remain stable after the second postnatal week. Mitral cell apical dendrites increase in length and complexity during the first few postnatal weeks (30). However, apical dendritic filtering could not account for the decrease in coupling coefficients, because we observed similar developmental decreases using paired dendritic recordings (15.5 ± 2.0%, P7–10, n = 14; 6.3 ± 0.8%, P14–35, n = 16; $P < 0.001$; Fig. S1).

Between the first and second week, the olfactory mucosa increases 2.5-fold in surface area, and the number and size of glomeruli increase similarly (30). Because coupling coefficients declined during this period of rapid olfactory development, we wondered whether sensory experience might affect electrical transmission. To address this issue, we deprived mice of sensory input using permanent unilateral naris occlusion on P1. Naris occlusion prevents odorant responses, acutely attenuates neural activity in the olfactory bulb, and uncouples cellular activity from the respiratory cycle (31). Naris occlusion was deemed successful when the bulb ipsilateral to the occlusion was smaller than the contralateral bulb after P28 (Fig. 1C) (32). Coupling coefficients between mitral cells in deprived bulbs (P > 28) did not show a developmental decrease, remaining as high (10.5 ± 1.4%, n = 22; Fig. 1D) as those in control animals at P7–10. In contrast, recordings in the contralateral bulbs
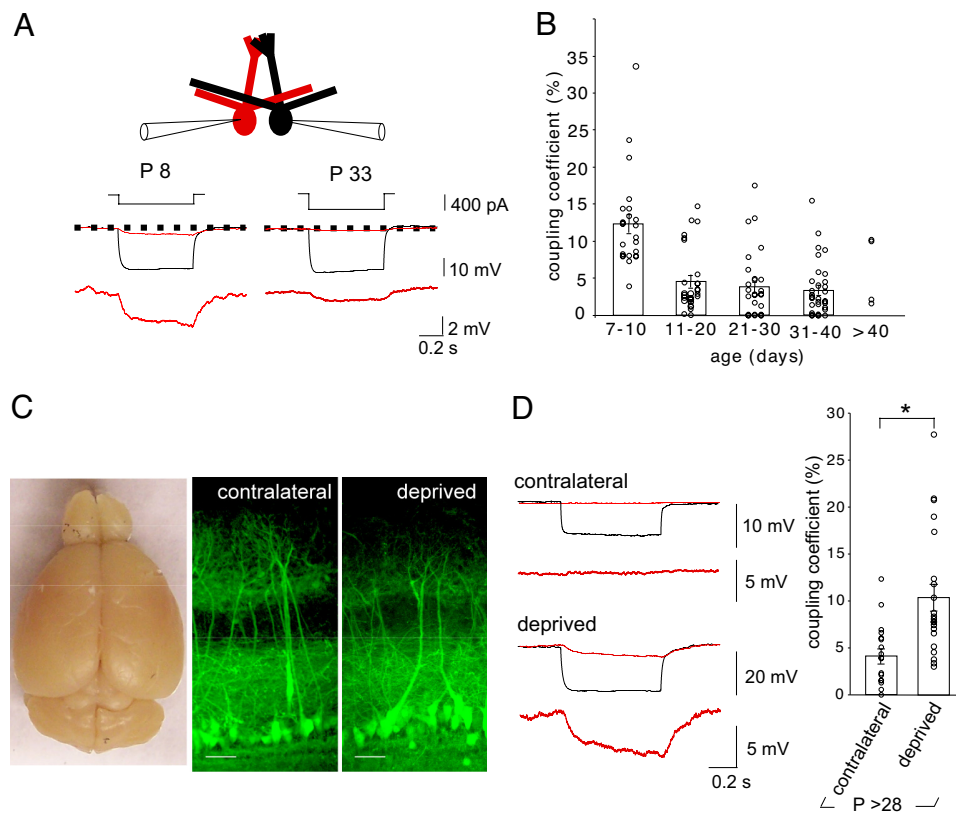

NEUROSCIENCE

Fig. 1. Sensory deprivation prevents the developmental decrease in coupling coefficients and alters olfactory bulb development. (*A*) Diagram of whole-cell somatic recordings from pairs of mitral cells that project to the same glomerulus. Hyperpolarizing current injections (range −250 to −400 pA, 0.7 s) into cell 1 (black) elicited a voltage deflection in the cell 2 (red). Each trace represents an average of 7–10 sweeps. Mitral cells at P8 showed higher coupling than at P33. (*B*) The coupling coefficient (ratio of the hyperpolarization in the test/stimulated cell) decreased after P10. (*C*) The right olfactory bulb was smaller in this P32 mouse after right naris occlusion at P1. The laminar organization of the olfactory bulb and the projection of apical dendrites to glomeruli were not altered in sensory-deprived animals. The images show slices from contralateral and sensory-deprived bulbs (P > 28), in which Thy1-YFP is expressed in a proportion of mitral cells. (Scale bar, 50 μm.) (*D*) In young adult mice (P > 28), the coupling coefficient was greater on the side that was sensory deprived. In the example contralateral control bulb shown, a hyperpolarizing current injection (−400 pA, 0.7 s) into cell 1 (black) elicited only a small voltage deflection in cell 2 (red), compared with the larger voltage deflection elicited in the deprived bulb (P < 0.001).

showed the expected decrease (4.1 ± 0.8% $n = 18$; $P < 0.001$, deprived vs. contralateral; Fig. 1*D*).

One month of sensory deprivation did not lead to any gross rearrangements in the lamination of the olfactory bulb, or the glomerular projection of mitral cells (Fig. 1*C*) (33). However, mitral cells from sensory-deprived animals had proportionately shorter apical dendrites and smaller glomerular diameters, consistent with impaired morphological development (Fig. 1*C*; Fig. S2). In contrast, genetic deletion of Cx36, which reduces the response of the glomerular circuit to afferent stimulation (27), did not affect dendritic growth (Fig. S2). Thus, sensory experience is necessary for the developmental decrease in coupling coefficients and morphological development of the glomerular circuit.

Coupling Coefficients and the Membrane Conductance. The decrease in coupling coefficients with development and their dependence on sensory experience could result from decreased expression of Cxs. However, Cx36 mRNA levels remain high in the olfactory bulb into adulthood, unlike the decreases observed in many brain regions (16, 34). Furthermore, coupling coefficients also depend on the non-gap-junctional membrane conductance (35, 36). We assessed the non-gap-junctional membrane conductance by comparing mitral cell input resistances and coupling coefficients in sensory-deprived animals, Cx36$^{-/-}$ animals, and control animals. In control animals, the input resistance markedly declined after the 1st postnatal week, a pattern similar to the decrease in coupling coefficients. In

contrast, the input resistances in mitral cells from young adult sensory-deprived and Cx36$^{-/-}$ mice were higher than in contralateral bulbs or in age-matched controls (Fig. 2*A*). As expected, electrical coupling was absent in mitral cell pairs from Cx36$^{-/-}$ mice (Fig. 2 *B* and *C*) (21).

To separate the contribution of gap junctions and the non-gap-junctional membrane conductance to the total membrane conductance, we simulated a glomerular network. We also examined the effect of carbenoxolone (CBX) on input resistance. The simulated network contained 15 mitral cells, each connected to other mitral cells by gap junctions (*SI Appendix*). The simulations incorporated the observed input resistances and coupling coefficients, and changes resulting from sensory deprivation (Fig. S3). The simulations predicted that the increase in membrane conductance during development is sufficient to account for the decrease in coupling coefficients. Random variability (uniform or biased) in the strength of the simulated connections did not alter this conclusion (Eqs. **S7** and **S8** in *SI Appendix*). For experiments examining CBX-treated cells, membrane conductance was considered as the residual (unblocked) conductance, whereas the estimate of the gap-junctional conductance was the portion blocked by CBX taking into account the differences in driving force (Eq. **s3.1** in *SI Appendix*). The calculated gap-junctional conductance did not change between P7–10 and >P28 (3.7 ± 0.9 nS vs. 4.5 ± 1.2 nS, $P = 0.59$, $n = 6$ for both groups). In contrast, there was a marked increase in the membrane conductance during the same period (9.9 ± 1.1 nS vs.

Fig. 2. Sensory deprivation and genetic deletion of Cx36 prevent developmental changes in membrane conductance. (*A*) Input resistance decreased in control mitral cells for all time intervals after P7–10 including the contralateral control group ($P < 0.001$). In contrast, input resistance for the sensory-deprived and Cx36$^{-/-}$ animals was much higher than the contralateral bulbs or age-matched controls, respectively ($P < 0.001$, $P < 0.002$). (*B* and *C*) As expected, in Cx36$^{-/-}$ animals a current pulse caused a hyperpolarization in one cell (black trace), but no electrical coupling in the follower cell (red trace). The confocal image shows 2 biocytin-filled mitral cells from a Cx36$^{-/-}$ mouse (P34). The margin of the glomerulus is outlined by the dotted line. (Scale bar, 50 μm.)

16.7 ± 1.4 nS, $P = 0.003$, $n = 6$ for both groups). The decrease of input conductance in CBX confirmed the prediction of the simulations (Fig. S3). Thus, gap-junctional conductance did not change substantially with age or sensory deprivation (Fig. S3*B*), whereas the genetic removal of Cx36 or sensory deprivation prevented the maturational increase in non-gap-junctional membrane conductance.

Maturation of the Circuit Reveals a Mitral–Mitral EPSC. The increase in membrane conductance during development should reduce the impact of electrical coupling. We tested this issue by examining transient responses to backpropagating actions potentials (bAPs) in

mitral cell pairs that projected to the same glomerulus. At P7–10, a bAP in cell 1 (bottom black trace in Fig. 3*A*) produced a transient inward current in cell 2 (upper red trace in Fig. 3*A*) that was blocked by CBX (middle red trace in Fig. 3*A*), but not by 2,3-dihydroxy-6-nitro-7-sulfonyl-benzo[*f*]quinoxaline (NBQX; $n = 10$, upper red trace in Fig. 3*A*). When we stimulated in the opposite direction (Fig. 3*A Right*), a bAP in cell 2 (red traces) produced a transient inward current in cell 1 (black traces). CBX abolished the transient inward current ($n = 10$, middle black trace in Fig. 3*A*). The bidirectional response and the block by CBX (Fig. 3*B*) are consistent with direct coupling of the action potential waveform through gap junctions in the absence of measurable chemical transmission. NBQX did not affect the peak amplitude of the transient (right upper black traces in Fig. 3*A*), but it did variably reduce a small, slow component ($n = 10$, range 12–85% of charge).

The situation was much different in mitral cells from young adult mice ($P > 28$). A single bAP now generated a large and rapid inward current in all cell pairs that was completely blocked by NBQX, indicative of chemical transmission (Fig. 3 *C Left* and *D*). We restricted our analysis to pairs of cells in which the apical dendrites were visualized and projected to the same glomerulus. Unlike the bidirectional coupling of action potential waveforms at P7–10, a bAP in the other cell did not evoke an EPSC (50 of 53 pairs Fig. 3*C Right*). The unidirectional mitral–mitral EPSCs did not depend on electrical transmission through gap junctions, because coupling coefficients for these cell pairs were similar in both directions ($4.8 \pm 1.3\%$ vs. $3.1 \pm 0.9\%$; $P = 0.12$, $n = 16$). The unidirectional mitral–mitral EPSC amplitude was 60.0 ± 6.4 pA ($n = 37$, P15–39).

The NBQX-sensitive mitral–mitral EPSCs were only seen in pairs of mitral cells that projected to the same glomerulus. Thus, the closely associated dendritic tufts within a glomerulus are the most likely synaptic site (37). Consistent with this idea, in dendritic recordings of electrically coupled mitral cells ($P > 28$, $n = 22$), a bAP produced a large EPSP in the other dendrite, whereas a subthreshold depolarizing pulse (1.2 nA, 5 ms) caused a barely detectable depolarization (Fig. S4). Similar to somatic recordings, the dendritic EPSP was unidirectional in all cases (upper black trace in Fig. S4). These results indicate that direct chemical transmission

Fig. 3. A mitral–mitral EPSC emerges in young adult animals. (*A* and *B*) For electrically coupled cell pairs at P7–10, a bAP elicited by a 1-ms current injection (bottom traces) produced a capacitive artifact followed by an inward current (top 2 traces). CBX (100 μM) abolished the NBQX-insensitive inward currents (middle traces), consistent with electrical coupling of the bAP. AP5 (100 μM) and gabazine (5 μM) were included in the extracellular solution. In some cases, NBQX (10 μM) decreased the slow component of the inward current (black cell; *Right Top*), but had no effect on the peak inward current (red cell; *Left*). (*C*) In contrast, for mitral cells at $P > 28$, short current injection (2.5–3.5 nA, 1 ms) elicited a bAP in cell 1 (red trace, *Left Bottom*) that produced an EPSC in cell 2 (black trace; *Left Top*) that was completely blocked by NBQX (10 μM; *Left Middle*). The EPSC was unidirectional as current injection in cell 2 elicited a bAP (black trace; *Right Middle*), but did not produce an EPSC in cell 1 (red trace; *Right Top*). At increased gain (right bottom traces), the cell shows only a capacitive transient. AP5 (100 μM) and gabazine (5 μM) were present in the extracellular solution. (*D*) NBQX completely blocked mitral–mitral EPSCs in young adult animals (14 of 14 pairs, $P < 0.0001$). All traces are averages of 7–10 consecutive sweeps.

Maher et al.

develops between mitral cells projecting to the same glomerulus by 1 month postnatal.

Properties of Mitral–Mitral EPSCs. As expected for chemical transmission, decreasing extracellular Ca^{2+} from 2 mM to 0.75 mM reduced the EPSC amplitude ($23 \pm 2\%$ of control amplitude, $n = 4$; $P < 0.0001$; Fig. S5 *Ai* and *Aii*) and increased the paired-pulse ratio (0.50 ± 0.06 vs. 0.94 ± 0.17, $n = 4$; $P < 0.05$; Fig. S5*Aiii*). Mitral–mitral EPSCs showed more paired-pulse depression compared with transmission between the same presynaptic mitral cell and a periglomerular cell [paired-pulse ratio (PPR) = 0.53 ± 0.04, $n = 6$, vs. 0.80 ± 0.06, interstimulus interval (ISI) 100 ms, $n = 7$; Fig. S5 *C and D*], suggesting that mitral cells may contain release sites with different properties. The paired pulse depression for mitral–mitral EPSCs appeared to be presynaptic because cyclothiazide (CTZ), which reduces AMPA receptor desensitization, did not affect the paired pulse ratio (0.70 ± 0.04 vs. 0.71 ± 0.05, ISI 100 ms, $n = 6$). However, as expected, CTZ did increase the EPSC amplitude and duration ($172 \pm 21\%$ control, $P < 0.02$; decay time constant: control 6.7 ± 0.4 ms, CTZ 14.4 ± 1.9 ms, $P < 0.01$, $n = 6$).

AMPA autoreceptor potentials, which result from direct activation of AMPA receptors on the mitral cell dendrite that released glutamate, were present in both cells (Fig. S5*B*), even though the mitral–mitral EPSC in these cell pairs was unidirectional. Thus, electrical coupling of the AMPA autoreceptor potential (19) is not a sufficient explanation for the mitral–mitral EPSC. Although block of glutamate uptake with DL-*threo*-β-benzyloxyaspartic acid (TBOA) can induce glutamate spillover within a glomerulus (24, 27), TBOA did not enhance the mitral–mitral EPSC (amplitude $77 \pm 9\%$ of control; $P > 0.05$, $n = 6$). The paired pulse ratio was also unaffected by TBOA ($0.67 \pm .04$ vs. $0.63 \pm .08$, $n = 6$, $P > 0.05$). Overall, these observations indicate that the mitral–mitral EPSC results from direct synaptic contacts.

Neural Activity in Sensory Deprived or Cx36$^{-/-}$ Mice. Our results indicate that the functional maturation of the glomerular circuit results in a functional decrease in electrical coupling, an increase in dendritic length and glomerular diameter, and the appearance of a mitral–mitral EPSC. To examine whether these processes were linked to neural activity, we compared the spontaneous electrical activity in slices from sensory-deprived animals with the activity in slices from Cx36$^{-/-}$ animals, which are known to have reduced excitability within the olfactory bulb (27). Brain slices of course lack the normal afferent input. However, spontaneous synaptic potentials and action potentials, and gap junctions, create a background level of electrical activity that serves as a measure of the overall excitability of the network. Surprisingly, spontaneous mitral cell activity in sensory-deprived animals ($n = 22$) was actually greater than in age-matched ($P > 28$) controls ($n = 18$, $P < 0.01$; Fig. 4 *A* and *B*). In contrast, spontaneous activity in mitral cells in Cx36$^{-/-}$ animals ($n = 8$) was as low as in the presence of synaptic receptor blockers ($P > 28$, $P = 0.78$, $n = 10$; Fig. 4 *A* and *B*). Mitral–mitral EPSCs were present and of similar amplitude in the deprived bulb (33.1 ± 6.8 pA, deprived bulb, $n = 9$; 50.8 ± 10.1 pA, control bulb, $n = 10$; $P = 0.3$; Fig. 4), but there were no detectable mitral–mitral EPSCs in Cx36$^{-/-}$ animals ($n = 8$ of 8; Fig. 4*C*). These observations indicate that spontaneous activity is not sufficient to drive functional maturation of the circuit, and that Cx36-mediated gap junctions are required for development of the mitral–mitral EPSC.

Discussion

Cx36, Coupling Coefficients, and Membrane Conductance. Cx36-mediated gap junctions between neurons are prominent during development (38), but their possible instructive roles in circuit formation are not well understood. In some circuits, gap junctions
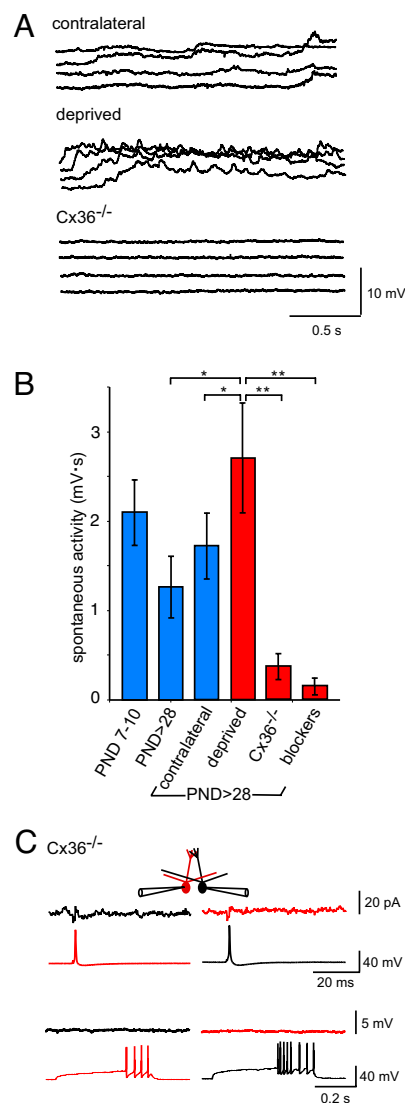
Fig. 4. Spontaneous mitral cell activity in sensory-deprived and Cx36$^{-/-}$ animals. (*A*) In young adult animals ($P > 28$) that underwent unilateral naris occlusion on P1, there was surprisingly robust spontaneous activity in the sensory-deprived bulb. The traces show 4 representative 2-s epochs of activity for 1 mitral cell. In contrast, an age-matched mitral cell from a Cx36$^{-/-}$ (undeprived) animal had very little spontaneous activity. (*B*) Spontaneous activity was integrated (mV-sec) for mitral cells in the groups of animals shown after determining a baseline during a quiescent period for each cell, before the period of data collection. As discussed in the text, spontaneous activity was actually somewhat greater in the deprived bulb than in age-matched controls, whereas in Cx36$^{-/-}$ mice, it was reduced to the same degree as by addition of NBQX, AP5, and gabazine (blockers). (*C*) Mitral–mitral EPSCs were not present in Cx36$^{-/-}$ mice. Short and long current injections elicited single bAPs or bursts of bAPs, respectively, in either mitral cell (bottom traces), but no synaptic current was present in the corresponding postsynaptic mitral cell (top traces; $n = 8$). The small response represents capacitive coupling. All traces represent an average of 7–10 consecutive sweeps.

essentially disappear in the adult (7, 39–42). Our results indicate that Cx36-mediated gap junctions persist into adulthood in the olfactory bulb. However, the impact at the soma of electrical coupling was decreased because of a maturational increase in non-gap-junctional membrane conductance. In young animals, the high coupling coefficients and low membrane conductance promote efficient coupling of electrical activity.

Our estimates of gap-junctional conductance and non-gap-junctional membrane conductance were based on simulations of a

glomerular network and on block of gap junctions with CBX. Caveats to be considered are potential nonspecific effects of CBX. For example, in cultured hippocampal neurons, CBX can cause small decreases in non-gap-junctional membrane resistance (ca 20%; see ref. 72). Such changes would cause a small underestimate of the gap-junctional conductance. Likewise, the simulations did not consider variables such as voltage-dependent conductances and their cellular distribution. For example, the electrical isolation of gap junctions in the apical tuft would cause the simulations to underestimate the gap-junctional conductance (43). However, the consistency between the approaches supports the conclusion that, during mitral cell development, it is the membrane conductance, not the gap-junctional conductance, which underlies the reduced impact of electrical transmission.

Mitral–Mitral EPSCs, Are They Really Synapses? Mitral–mitral excitation largely has been attributed to spillover or coupling of autoexcitatory potentials through gap junctions (19, 24), but recent studies indicate the possibility of excitatory synapses between mitral cells (37, 44). The properties of mitral–mitral EPSCs in our experiments leave little doubt that they arise from direct synaptic interactions, and are limited to older animals; thus, explaining the lack of such EPSCs in earlier data using slices from PN14–21 animals (19, 27). These properties include the block by an AMPA receptor antagonist, the dependence on extracellular calcium, and the presence of typical calcium-dependent paired pulse depression. Also, EPSCs were virtually always generated in only one direction in pairs of mitral cells, which is incompatible with electrical transmission in cells of comparable impedance (45). Although the location of the presynaptic site remains to be established, EPSCs were only present in cell pairs that project to the same glomerulus. This observation suggests a dendritic release site within a glomerulus (44). We cannot completely exclude nonglomerular contacts such as synapses between lateral and apical dendrites or the presence of recurrent mitral cells axons, but mitral cell axon collaterals have not been reported in the external plexiform or glomerular layer (46).

Mitral–mitral EPSCs could result from glutamate spillover at conventional mitral-interneuronal synapses (47), or from distinct release sites. We favor the latter for several reasons. First, spillover should be enhanced by block of glutamate uptake, but no such enhancement occurred in our experiments. Although there is no ultrastructural evidence for conventional synapses between rodent mitral cell dendrites (48–50), clear vesicles are scattered along apical dendrites (48). Asymmetric synapses have also been noted between salamander mitral cell dendrites (51). Last, the difference in short-term plasticity between the mitral–mitral EPSC and the mitral-interneuron EPSC may suggest distinct release sites.

Experience-Dependent Maturation of the Glomerular Circuit. Olfactory input reaches the olfactory bulb before birth (52); thus, the postnatal maturation of the glomerular circuit is subject to the influence of sensory input, as well as local circuit activity. Such influences are well known to have a crucial role in the refinement of developing sensory circuits (1, 53). Maturation of visual and somatosensory circuits continues for weeks after the onset of sensory input, and sensory deprivation leads to abnormal circuit structure and function (3). In the olfactory bulb, naris occlusion has been used to induce sensory deprivation. Naris occlusion can cause reduction in the size of glomerular tufts, a reduction in dopamine content, and possible synaptic rearrangements (54–56).

Although acute naris occlusion reduces spontaneous and odor-evoked spiking in mitral cells (31), our results show a more complex activity pattern in animals that were sensory-deprived for the first month of life. Despite the loss of patterned sensory input, spontaneous activity in the deprived bulb was actually larger than the

contralateral control, to which the higher degree of electrical coupling likely contributes. This observation may explain the increased deoxyglucose signals in response to odorants in animals in which the naris is reopened after chronic deprivation (57). However, the residual spontaneous activity in deprived animals was not sufficient to drive the morphological development or functional maturation of the glomerular circuit. Without sensory input, the morphology and membrane properties of mitral cells seem to be arrested at the initial stage of glomerular formation (i.e., P7–10).

Necessary Role of Cx36 in Circuit Maturation. Our results indicate that genetic removal of Cx36-mediated gap junctions prevents the development of chemical transmission between mitral cells. Developmental interactions between electrical and chemical transmission also occur in some invertebrate systems. For example in *Drosophila* optic lamina mutations in gap junction genes (innexins) can prevent chemical transmission between retinal neurons and lamina monopolar neurons (58). In other cases, invertebrate systems show transitions in either direction between electrical coupling and chemical transmission (59, 60). A relationship between decreases in electrical coupling and increases in chemical transmission has also been reported in the ferret visual cortex (61). Synaptic activity may in some cases affect electrical coupling as well (62–65).

Why gap junctions are required is not clear. Compensatory changes can occur in knockout animals (66); thus, further experiments will be necessary to examine the mechanism by which Cx36 affects synapse development. Electrical synapses could certainly provide important biochemical and/or electrical signaling between mitral cells, which could instruct pre or postsynaptic orientation and the proper delivery of synaptic molecules. Alternatively, gap junctions may act as molecular staples, bringing neighboring dendrites into close proximity to allow for chemical signaling. In support of the latter hypothesis, mitral cells in Cx36$^{-/-}$ mice are capable of dendritic glutamate release (27), but our results show that they do not have mitral–mitral EPSCs. Also, synchronized oscillations are only present in Cx36$^{-/-}$ mice when glutamate transporters are blocked. These results suggest that dendrites may not be as closely apposed in the absence of gap junctions (66).

Functional Consequences. Odor discrimination of 2 structurally similar chemicals can occur rapidly, in <200 ms, the equivalent of 1 sniff (67). Synchronization of mitral cells within a glomerulus is one potential mechanism to support such rapid olfactory processing. Although synchronization has been largely attributed to electrical coupling in young animals, the excitatory chemical transmission we describe here should enhance synchronization of mitral cells as the circuit matures. Apical dendritic tufts are capable of local generation of sodium-dependent action potentials with strong stimulation of olfactory receptor neurons (ORNs) (68, 69). Thus, rapid synchronization of glomerular output can occur in the apical tuft without requiring bAPs. Because there are ≈15–20 mitral cells per glomerulus in the mouse (70), closely spaced afferent inputs are likely to lead to rapid synchronization within the apical tuft. Given the strong synaptic depression of mitral–mitral EPSCs, we suggest that they provide a phasic response to strong odorant stimulation.

Methods

Tissue Preparation. All animal protocols were approved by the Institutional Animal Care and Use Committee and followed the National Institutes of Health guidelines for the ethical treatment of animals. Olfactory bulb slices were prepared from 7- to 42-day-old Thy-1 transgenic mice that expressed YFP in a subset of mitral/tufted cells (line YFP-G) (71). All recordings were done at 31–34 °C. We used exclusively mitral cell pairs that projected to the same glomerulus. Detailed protocols for electrophysiology, immunohistochemistry, and morphological measurements are included in *SI Methods*. For some experiments, the right naris was occluded by electrocauterization as described in *SI Methods*. Naris occlusion prevents stimuli from reaching the olfactory epithelium, but does not directly

damage olfactory receptor neurons or their axons that innervate the olfactory bulb.

Network Modeling. We simulated a glomerular network of mitral cells connected by gap junctions using Matlab 6.5 (MathWorks, 2002). Matrices with random entries were generated using the Matlab function, rand. For additional details, see *SI Appendix* and Fig. S3.

Data Analysis and Statistics. We used AxoGraph on a Macintosh computer for analysis. Estimates of charge for spike-coupled inward currents were mea-

sured by integrating the currents starting at the onset of the response. For all experiments, statistical significance was determined by using standard *t* tests and Newman–Keuls 1-way ANOVA, and indicated on the figures with asterisks. Averaged data values are reported as mean $\pm$ SEM.

1. Katz LC, Shatz CJ (1996) Synaptic activity and the construction of cortical circuits. *Science* 274:1133–1138.
2. Grubb MS, Thompson ID (2004) The influence of early experience on the development of sensory systems. *Curr Opin Neurobiol* 14:503–512.51.
3. Fox K, Wong RO (2005) A comparison of experience-dependent plasticity in the visual and somatosensory systems. *Neuron* 48:465–477.
4. Bennett MVL, et al. (1991) Gap junctions: New tools, new answers, new questions. *Neuron* 6:305–320.
5. Roerig B, Feller MB (2000) Neurotransmitters and gap junctions in developing neural circuits. *Brain Res Brain Res Rev* 32:86–114.
6. Yuste R, Peinado A, Katz LC (1992) Neuronal domains in developing neocortex. *Science* 257:665–669.
7. Peinado A, Yuste R, Katz LC (1993) Gap junctional communication and the development of local circuits in neocortex. *Cereb Cortex* 3:488–498.
8. Strata F, et al. (1997) A pacemaker current in dye-coupled hilar interneurons contributes to the generation of giant GABAergic potentials in developing hippocampus. *J Neurosci* 17:1435–1446.
9. Milner LD, Landmesser LT (1999) Cholinergic and GABAergic inputs drive patterned spontaneous motoneuron activity before target contact. *J Neurosci* 19:3007–3022.
10. Wong RO (1999) Retinal waves and visual system development. *Annu Rev Neurosci* 22:29–47.
11. Garaschuk O, Linn J, Eilers J, Konnerth A (2000) Large-scale oscillatory calcium waves in the immature cortex. *Nat Neurosci* 3:452–459.
12. Ben-Ari Y (2001) Developing networks play a similar melody. *Trends Neurosci* 24:353–360.
13. Condorelli DF, et al. (1998) Cloning of a new gap junction gene (Cx36) highly expressed in mammalian brain neurons. *Eur J Neurosci* 10:1202–1208.
14. Sohl G, Maxeiner S, Willecke K (2005) Expression and functions of neuronal gap junctions. *Nat Rev Neurosci* 6:191–200.
15. Hestrin S, Galarreta M (2005) Electrical synapses define networks of neocortical GABAergic neurons. *Trends Neurosci* 28:304–309.
16. Hormuzdi SG, et al. (2001) Impaired electrical signaling disrupts gamma frequency oscillations in connexin 36-deficient mice. *Neuron* 31:487–495.
17. Maier N, et al. (2002) Reduction of high-frequency network oscillations (ripples) and pathological network discharges in hippocampal slices from connexin 36-deficient mice. *J Physiol* 541:521–528.
18. Landisman CE, et al. (2002) Electrical synapses in the thalamic reticular nucleus. *J Neurosci* 22:1002–1009.
19. Schoppa NE, Westbrook GL (2002) AMPA autoreceptors drive correlated spiking in olfactory bulb glomeruli. *Nat Neurosci* 5:1194–1202.
20. Buhl DL, Harris KD, Hormuzdi SG, Monyer H, Buzsaki G (2003) Selective impairment of hippocampal gamma oscillations in connexin-36 knock-out mouse in vivo. *J Neurosci* 23:1013–1018.
21. Christie JM, et al. (2005) Connexin36 mediates spike synchrony in olfactory bulb glomeruli. *Neuron* 46:761–772.
22. Nicoll RA, Jahr CE (1982) Self-excitation of olfactory bulb neurones. *Nature* 296:441–444.
23. Aroniadou-Anderjaska V, Ennis M, Shipley MT (1999) Dendrodendritic recurrent excitation in mitral cells of the rat olfactory bulb. *J Neurophysiol* 82:489–494.
24. Isaacson JS (1999) Glutamate spillover mediates excitatory transmission in the rat olfactory bulb. *Neuron* 23:377–384.
25. Salin PA, Lledo PM, Vincent JD, Charpak S (2001) Dendritic glutamate autoreceptors modulate signal processing in rat mitral cells. *J Neurophysiol* 85:1275–1282.
26. Schoppa NE, Westbrook GL (2001) Glomerulus-specific synchronization of mitral cells in the olfactory bulb. *Neuron* 31:639–651.
27. Christie JM, Westbrook GL (2006) Lateral excitation within the olfactory bulb. *J Neurosci* 26:2269–2277.
28. Schoppa NE, Urban NN (2003) Dendritic processing within olfactory bulb circuits. *Trends Neurosci* 26:501–506.
29. Franks KM, Isaacson JS (2005) Synapse-specific downregulation of NMDA receptors by early experience: A critical period for plasticity of sensory input to olfactory cortex. *Neuron* 47:101–114.
30. Pomeroy SL, LaMantia AS, Purves D (1990) Postnatal construction of neural circuitry in the mouse olfactory bulb. *J Neurosci* 10:1952–1966.
31. Philpot BD, Foster TC, Brunjes PC (1997) Mitral/tufted cell activity is attenuated and becomes uncoupled from respiration following naris closure. *J Neurobiol* 33:374–386.
32. Brunjes PC (1994) Unilateral naris closure and olfactory system development. *Brain Res Brain Res Rev* 19:146–160.
33. Matsutani S, Yamamoto N (2000) Differentiation of mitral cell dendrites in the developing main olfactory bulbs of normal and naris-occluded rats. *J Comp Neurol* 418:402–410.
34. Belluardo N, et al. (2000) Expression of connexin36 in the adult and developing rat brain. *Brain Res* 865:121–138.
35. Bennett MVL (1977) The nervous system, Part I. *Handbook of Physiology*, eds Brookhart JM, Mountcastle VB (Am Physiol Soc, Bethesda), Sect 1, pp 357–416.
36. Amitai Y, et al. (2002) The spatial dimensions of electrically coupled networks of interneurons in the neocortex. *J Neurosci* 22:4142–4152.
37. Urban NN, Sakmann B (2002) Reciprocal intraglomerular excitation and intra- and interglomerular lateral inhibition between mouse olfactory bulb mitral cells. *J Physiol* 542:355–367.

38. Sutor B, Hagerty T (2005) Involvement of gap junctions in the development of the neocortex. *Biochim Biophys Acta* 1719:59–68.
39. Connors BW, Benardo LS, Prince DA (1983) Coupling between neurons of the developing rat neocortex. *J Neurosci* 3:773–782.
40. Walton KD, Navarrete R (1991) Postnatal changes in motoneurone electronic coupling studied in the in vitro rat lumbar spinal cord. *J Physiol* 433:283–305.
41. Sohl G, Degen J, Teubner B, Willecke K (1998) The murine gap junction gene connexin36 is highly expressed in mouse retina and regulated during brain development. *FEBS Lett* 428:27–31.
42. Degen J, et al. (2004) Expression pattern of lacZ reporter gene representing connexin36 in transgenic mice. *J Comp Neurol* 473:511–525.
43. Migliore M, Hines ML, Shepherd GM (2005) The role of distal dendritic gap junctions in synchronization of mitral cell axonal output. *J Comp Neurosci* 18:151–161.
44. Pimental DO, Margrie TW (2008) Glutamatergic transmission and plasticity between olfactory bulb mitral cells. *J Physiol* 586:2107–2119.
45. Johnston D, Wu M (1995) *Foundations of Cellular Neurophysiology* (MIT Press, Cambridge, MA).
46. Orona E, Rainer EC, Scott JW (1984) Dendritic and axonal organization of mitral and tufted cells in the rat olfactory bulb. *J Comp Neurol* 226:346–356.
47. Shepherd GM (1972) Synaptic organization of the mammalian olfactory bulb. *Physiol Rev* 52:864–917.
48. Price JL, Powell TP (1970) The mitral and short axon cells of the olfactory bulb. *J Cell Sci* 7:631–651.
49. Pinching AJ, Powell TP (1971) The neuropil of the glomeruli of the olfactory bulb. *J Cell Sci* 9:347–377.
50. White EL (1972) Synaptic organization in the olfactory glomerulus of the mouse. *Brain Res* 37:69–80.
51. Allen DM, Hamilton KA (2000) Ultrastructural identification of synapses between mitral/tufted cell dendrites. *Brain Res* 860:170–173.
52. Hinds JW (1968) Autoradiographic study of histogenesis in the mouse olfactory bulb. II. Cell proliferation and migration. *J Comp Neurol* 134:305–322.
53. Del Rio T, Feller MB (2006) Early retinal activity and visual circuit development. *Neuron* 52:221–222.
54. Baker H, Morel K, Stone DM, Maruniak JA (1993) Adult naris closure profoundly reduces tyrosine hydroxylase expression in mouse olfactory bulb. *Brain Res* 614:109–116.
55. Philpot BD, Men D, McCarty R, Brunjes PC (1998) Activity-dependent regulation of dopamine content in the olfactory bulbs of naris-occluded rats. *Neuroscience* 85:969–977.
56. Leon M (1998) Compensatory responses to early olfactory restriction. *Ann NY Acad Sci* 855:104–108.
57. Guthrie KM, Wilson DA, Leon M (1990) Early unilateral deprivation modifies olfactory bulb function. *J Neurosci* 10:3402–3412.
58. Curtin KD, Zhang Z, Wyman RJ (2002) Gap junction proteins expressed during development are required for adult neural function in the Drosophila optic lamina. *J Neurosci* 22:7088–7096.
59. Szabo TM, Faber DS, Zoran MJ (2004) Transient electrical coupling delays the onset of chemical neurotransmission at developing synapses. *J Neurosci* 24:112–120.
60. Leitch B, Cobb JL, Heitler WJ, Pitman RM (1989) Post-embryonic development of rectifying electrical synapses in the crayfish: Ultrastructure. *J Neurocytol* 18:749–761.
61. Kandler K, Katz LC (1998) Relationship between dye coupling and spontaneous activity in developing ferret visual cortex. *Dev Neurosci* 20:59–64.
62. Mentis GZ, Diaz E, Moran LB, Navarrete R (2002) Increased incidence of gap junctional coupling between spinal motoneurones following transient blockade of NMDA receptors in neonatal rats. *J Physiol* 544:757–764.
63. Pastor AM, Mentis GZ, De La Cruz RR, Diaz E, Navarrete R (2003) Increased electrotonic coupling in spinal motoneurons after transient botulinum neurotoxin paralysis in the neonatal rat. *J Neurophysiol* 89:793–805.
64. Arumugam H, Liu X, Colombo PJ, Corriveau RA, Belousov AB (2005) NMDA receptors regulate developmental gap junction uncoupling via CREB signaling. *Nat Neurosci* 8:1720–1726.
65. Urschel S, et al. (2006) Protein kinase A-mediated phosphorylation of connexin36 in mouse retina results in decreased gap junctional communication between AII amacrine cells. *J Biol Chem* 281:33163–33171.
66. De Zeeuw CI, et al. (2003) Deformation of network connectivity in the inferior olive of connexin36-deficient mice is compensated by morphological and electrophysiological changes at the single neuron level. *J Neurosci* 23:4700–4711.
67. Uchida N, Mainen ZF (2003) Speed and accuracy of olfactory discrimination in the rat. *Nat Neurosci* 6:1224–1229.
68. Chen WR, Midtgaard J, Shepherd GM (1997) Forward and backward propagation of dendritic impulses and their synaptic control in mitral cells. *Science* 278:463–467.
69. Zhou Z, et al. (2006) Dendritic excitability and calcium signalling in the mitral cell distal glomerular tuft. *Eur J Neurosci* 24:1623–1632.
70. Royet J-P, Distel H, Hudson R, Gervais R (1998) A re-estimation of the number of glomeruli and mitral cells in the olfactory bulb of rabbit. *Brain Res* 788:35–42.
71. Feng G, et al. (2000) Imaging neuronal subsets in transgenic mice expressing multiple spectral variants of GFP. *Neuron* 28:41–51.
72. Tovar KR, Maher BJ, Westbrook GL (2009) Direct actions of carbenoxolone on synaptic transmission and neuronal membrane properties. *J Neurophysiol* 102:974–978.